Internal Report ITeSRE 298/2000

October 2000

# PLANCK/LFI: SENSITIVITY ESTIMATES FOR THE DETECTION AND STUDY OF VARIABLE AND MOVING SOURCES

C. Burigana

*Istituto TeSRE/CNR, via P. Gobetti 101, I-40122 Bologna, Italy*

Internal Report ITeSRE 298/2000

October 2000

# PLANCK/LFI: SENSITIVITY ESTIMATES FOR THE DETECTION AND STUDY OF VARIABLE AND MOVING SOURCES

C. BURIGANA

*Istituto TeSRE/CNR, via P. Gobetti 101, I-40122 Bologna, Italy*

SUMMARY – The final sensitivity of the PLANCK surveyour maps of temperature fluctuations of the cosmic microwave background and of several astrophysical components, of galactic and extragalactic nature, will take advantage from the whole set of receivers and the full observation time. On the contrary, for the detection and/or the study of moving sources, like comets or asteroids, and of the study of the variability of some classes of sources, like active galaxies, we can take advantage only from the sensitivity of a limited number of receivers and/or for a limited time interval. Preliminary estimates of the PLANCK Low Frequency Instrument (LFI) sensitivity to these kinds of scientific purposes are here provided by taking into account the current optical design of the PLANCK telescope and focal plane unit, the LFI sensitivity and the particular way of PLANCK to observe the sky, the main astrophysical and cosmological source of confusion noise, and the possibility to use the previous observations of the MAP satellite. This work has been done in the framework of the PLANCK LFI activities.

## 1 Introduction: PLANCK LFI performances

The PLANCK surveyour [1] will observe the sky at nine frequencies with different angular resolutions and sensitivities; we report in Table 1 the relevant parameters for the PLANCK Low Frequency Instrument (LFI) (see columns 1, 4 and 5). The relative bandwidth of the LFI is $\simeq 20\%$ (see column 2 of Table 1).

We will refer here to the nominal PLANCK LFI sensitivity per resolution element (a squared pixel with side given equal to the Full Width at Half Maximum (FWHM) of the corresponding beam) as recently revised by the LFI Consortium (PLANCK Low Frequency Instrument, Instrument Science Verification Review, October 1999, LFI Design Report, private reference).

Fig. 1 shows a typical map of normalized sensitivity (i.e., the sensitivity divided by the averaged sensitivity of the observed pixels in the sky) for a PLANCK beam: note how the

[1] http://astro.estec.esa.nl/SA-general/Projects/Planck/

sensitivity increases with the module of the ecliptic latitude up to a ring of maximum sensitivity which contains a small unobserved sky region. This is shown in the Fig. 2, where we report the normalized sensitivity averaged over the ecliptic longitudes as function of the ecliptic colatitude (solid line): it is close to unit at the ecliptic colatitude $\theta_e \simeq 50°$ and 130° and is quite well approximated by the law $\sqrt{\sin\theta_e/\sin 50°}$ (dashed line). For completeness, we report also in Fig. 3 the fractions of sky area corresponding to different values of the normalized sensitivity. Of course, particularly for the sky regions close to the ecliptic poles, its detailed behaviour on $\theta_e$ depends on the choice of the scan angle $\alpha$, the adopted scanning strategy and the beam position on the telescope field of view.

Since we are here interested on the study of objects with variable position or flux, their detection/observation and/or the estimate of its flux can not take easily advantage from the twice covering of the sky in the 14 months of observations nor from the coadding of data from different feeds if they look at different sky positions at the same time.

In addition to the instrumental noise, the sky itself exibits a confusion noise given by the various galactic and extragalactic temperature fluctuations and from the cosmic microwave background (CMB) anisotropies, relevant at different angular scales $\theta \simeq 180°/\ell$, where $\ell$ is the multipole of the harmonic expansion of the temperature fluctuation pattern. We report in Table 1 the fluctuation level of the CMB anisotropy assuming a rms thermodynamic temperature fluctuation of about 95 $\mu$K as derived for a standard flat model approximately COBE/DMR normalized with cosmological parameters compatible with the present constraints on CMB fluctuations at moderate multipoles derived from recent balloon experiments; of course the accurate determination of the CMB confusion noise at small scales is the main PLANCK goal.

Then we report the extragalactic source confusion noise (by taking into account both radiosources and infrared sources), as evaluated by Toffolatti et al. (1998) and revised by De Zotti et al. (1999a,b). More precisely, in these estimates we compute the source confusion noise (in thermodynamic temperature fluctuations) as $\sigma_{ex.sou.} = \sqrt{C_l/(\mathrm{FWHM/rad})}$ where the angular power spectrum $C_l$ is the sum of the $C_l$ of radiosource fluctuations and far-IR source fluctuations (at LFI frequency radiosource fluctuations overwhelm far-IR source fluctuations), as quoted by De Zotti et al. (1999b) for a conservative detection limit of 1 Jy (see their Table 6). These estimates may be pessimistic, on the other hand it would be probably difficult to to subtract sources in real time with high accuracy.
The galactic fluctuation levels reported here are only indicative and refer to moderate and high galactic latitude, as large variations are present in the sky.

The relevant global sensitivity for point source detection/observation is typically assumed by the standard $\sigma$-clipping methods as the sum in quadrature of all the sources of confusion noise, multiplied by a proper constant (for example $n_c = 2$, 2.5, 3 or 5).

We report also in the last column of Table 1 the sensitivity of the MAP experiment [2] ($\sim 35\mu$K, in terms of thermodynamic temperature, on squared pixels with 0.3° side at each frequency channel, 22, 30, 40, 60 and 90 GHz), rescaled at the corresponding PLANCK beam size. In fact, we can argue that after the MAP mission, the sum of the CMB and foreground temperature fluctuation on each sky pixel will be known with the MAP accuracy; in this case, in the evaluation of the detection level for point source detection/observation we have to multiply by $n_c$ the sum in quadrature of the PLANCK and MAP sensitivities.

The relationship between rms noises and temperature fluctuations in terms of antenna temperature and thermodynamic temperature is $\Delta\delta T_{ant} = \Delta\delta T_{therm} x^2 \exp x/(\exp x - 1)^2$, where $x = h\nu/k/T_0$, $T_0 = 2.725$ K being the CMB monopole thermodynamic temperature as estabhlished by Mather et al. 1999. [The function $x^2\exp x/(\exp x - 1)^2$ is equal to $\simeq 0.977$, 0.951, 0.882 and 0.777 respectively at 30, 44, 70 and 100 GHz].

[2] http://map.gsfc.nasa.gov/html/

Table 1: Instrumental performances and confusion noise estimates for PLANCK LFI.

| $\nu_{\rm eff}$ (GHz) | Band (GHz) | $N_{rad}$ | FWHM (arcmin) | $\sigma_{\rm noise}$ ($\mu$K) | $\sigma_{\rm noise}$ (mJy) | $\sigma_{\rm CMB}$ (mJy) | $\sigma_{\rm ex.sou.}$ (mJy) | $\sigma_{\rm Gal}$ (mJy) | $\sigma_{\rm noise,MAP}$ (mJy) |
|---|---|---|---|---|---|---|---|---|---|
| 30 | 27.0÷33.0 | 4 | 33.6 | 5.1 | 13.4 | 245 | 59.1 | 100 | 48 |
| 44 | 39.6÷48.4 | 6 | 22.9 | 7.8 | 20.5 | 238 | 46.2 | 45 | 69 |
| 70 | 63.0÷77.0 | 12 | 14.4 | 10.6 | 28.0 | 221 | 31.5 | 15 | 102 |
| 100 | 90.0÷110.0 | 34 | 10.0 | 12.4 | 32.2 | 192 | 20.9 | 7 | 127 |

For a point source with flux $F_\nu$ observed with a beam response, $J$, normalized to the beam maximum response, the observed antenna temperature in given by

$$10^{-41}(c^2/2k)[(F_\nu/{\rm Jy})/(\nu/{\rm GHz})^2](J/\int_{4\pi} Jd\Omega)\,.$$

For a beam well approximated by a Gaussian shape $\int_{4\pi} Jd\Omega \simeq (\pi/4{\rm ln}2)({\rm FWHM/rad})^2$. We are interested here to sources with weak or moderate flux, i.e. essentially detectable only when they fall within a pixel with a side $\simeq$ FWHM about the beam centre. In the relationship between the antenna temperature and the flux reported here we simplify the beam response as unit within a pixel with a side $\simeq$ FWHM about the beam centre and null otherwhere, i.e. $\int_{4\pi} Jd\Omega) \simeq ({\rm FWHM/rad})^2$ [it is clear that, in reality, a source may be in principle observable at angles larger than $\simeq$ FWHM/2 from the beam centre with the corresponding beam response; this is in particular the case of bright sources, such as external planets that can be used for pattern reconstruction in-flight (see, e.g., Burigana et al. 2000)]. In this approximation, the relationship between the rms flux fluctuations and the rms antenna temperature fluctuations on a squared pixel with side $\Delta\theta$ ( $\simeq$ FWHM) is $\Delta\delta B_\nu/{\rm Jy} \simeq 30.7[\Delta\delta T_{ant}/{\rm mK}][\nu/{\rm GHz}]^2[\Delta\theta/{\rm rad}]^2$.

In the following sections we will derive the LFI sensitivity at the different channels relevant for the study of moving objects and variable sources from the PLANCK LFI time order data by appropriately rescaling the sensitivities of the final LFI maps. Since it would be possible to exploit the microwave maps derived from MAP data and cleaned at the level of MAP sensitivity from the effect of source flux variations at the epoch of MAP observations and from the tracts of moving objects, it is clear that in the worst case scenario the sensitivity levels relevant for the following discussions will be the sum in quadrature of the appropriately rescaled PLANCK sensitivities and of the sensitivities of the final maps of MAP. These will be also the sensitivities appropriate to the detection or study of moving objects and variable sources before the production of PLANCK maps. On the other hand, after the PLANCK data analysis and the production of the PLANCK cleaned frequency maps, we may be able to take advantage from the knowledge of the sky fluctuation in the positions of the considered variable sources or moving objects with a sensitivity approximately equal to the final sensitivity of PLANCK maps multiplied by $\sqrt{2}$, i.e. about a factor 2 better than MAP final sensitivity: this would be possible in the case of moving objects (that do not assume the same sky position in the subsequent PLANCK sky coverages) and in the case of a variable source in a quiescent phase during one of the PLANCK coverages of the corresponding sky region.

## 2 Beam location on the telescope field of view and scanning strategy

The LFI beams corresponding to the LFI feeds at different frequencies are located in a ring on the PLANCK telescope field of view, as shown in Fig. 4. The direction in the sky of the coordinate V is parallel to scan circle of the PLANCK telescope line of sight generated by the spacecraft rotation around its spin axis. The direction in the sky of the coordinate U, orthogonal to V, is, at least for simple scanning strategies (i.e., with the spacecraft spin axis always parallel to the antisolar direction), parallel to the spin axis shift direction during the mission. Note that each the LFI beam, except one beam at 100 GHz and at one 44 GHz, is symmetrically located to another LFI beam with respect to the axis V=0 , or, in other words, two beams observe the same scan circle at each spin axis repointing. The LFI array spans an angle, $\Delta\psi$, of about 7.5° in the U direction. Since the spacecraft spin axis is shifted by 2.5′ each hour, i.e. by 1° each day, at small ecliptic latitudes the PLANCK array spans a given meridian in about 7–8 days. More precisely, by considering the FWHM of the beams and their locations in the U direction, the set of the 44 GHz beams and of the 70 GHz beams cross a given meridian in about 18 hours, the two 30 GHz beams cross a given meridian in the beam (FWHM) travel time, $\sim$ 13 hours, and the set of 100 GHz beams cross a given meridian in about 5–6 days. The meridian travel time, $\tau(\theta_e)$, at ecliptic colatitudes $\theta_e$ different than $\simeq 90°$ is given by $\tau(\theta_e) \simeq \tau(90°)/\sin\theta_e$. This means that obiects located at high absolute ecliptic latitudes may be continuously observed for long times and with a sensitivity significantly better than the average. This points have direct implications for the observations of variable sources, a topic discussed in Sect. 4.

## 3 LFI sensitivity for moving sources

The LFI sensitivity relevant for the study of moving sources has to be appropriately rescaled with respect to that reported in Table 1 to include several factors of sensitivity degradation.

A first sensitivity degradation factor, $\sim \sqrt{2}$, derives by considering only a single sky coverage and provides a lower limit to the sensitivity relevant here (we neglect in the present estimates the small increase of this degradation factor with respect to the value $\sqrt{2}$ introduced by the limited sky regions observed three times duration the mission).

Another degradation factor, $\sqrt{N_{ric,sky}}$, where $N_{ric,sky}$, ranging from 2 to 17, is the number of radiometers per channel pointing at the same sky position at the same time, takes into account the displacement of the different receivers in the telescope field of view. In column 3 of Table 1 we report the number of LFI radiometers. For the LFI channels $N_{ric,sky} = N_{rad}/2 = N_{feed}$, because we have 2 radiometers per feed horn. On the other hand, in all the cases except for one feed at 100 GHz and one at 44 GHz, a pair of LFI feeds look the same scan circle in the sky, being located in the focal plane unit to follow the sky scan direction as the spacecraft spins. This factor, $\sqrt{N_{ric,sky}}$, taken into account in Table 2 at 44 and 100 GHz, provides then a pessimistic value for our sensitivity estimates; a factor more adequate for the majority of the cases, and taken into account in Table 2 at 30 and 70 GHz, is $\sqrt{N_{ric,sky}/2}$.

A last degradation factor $\sim \sqrt{\mathrm{FWHM}/\Delta\theta_s}$, where $\Delta\theta_s$ is the spin axis shift between two consecutive hours (2.5 arcmin), takes into account the possibility that a moving object falls out of the beam after a given spin axis repointing.

Table 2: Instrumental noise estimates for moving sources. The table values have to be multiplied by 1.15 for objects close to the ecliptic plane. The worst estimates provide also the averaged sensitivity (properly holding at $\theta_e \simeq 50°$ and 130°) for the study of source variability at short time-scales (few hours, see also Sect. 4).

| $\nu_{\rm eff}$/GHz | $\sigma_{\rm noise}/\mu$K | $\sigma_{\rm noise}$/mJy |
|---|---|---|
| 30 | 7.2÷26.4 | 19.0÷69.9 |
| 44 | 11.0÷75.8 | 29.0÷152.7 |
| 70 | 15.0÷62.3 | 39.6÷164.5 |
| 100 | 17.5÷144.6 | 45.5÷375.9 |

Taking into account all these sensitivity degradation factors, the nominal PLANCK sensitivities can be resumed in the ranges reported in Table 2; we provide these sensitivities in terms of antenna temperature and flux.

In practice, we have to take in mind that the interesting moving objects are generally located close to the ecliptic plane, where the PLANCK sensitivity is $\simeq 15\%$ worst than the averaged sensitivity (see Fig. 2). Therefore, the values reported in Table 2 have to be typically multiplied by $\simeq 1.15$.

# 4 LFI sensitivity for variable sources

The LFI sensitivity relevant for the to study of variable sources has to be appropriately rescaled with respect to that reported in Table 1 to include several factors of sensitivity degradation, in a way different from that described in the previous section.

Variable sources can be found at arbitrary directions in the sky. A variation in sensitivity by a factor $\sim 6$ in the different sky regions has then to be taken into account. We firstly consider here the case of sources at $\theta_e \sim 50°$ or 130°, where the normalized sensitivity is close to unit.

It is instructive to firstly consider the worst case of a single source transit on a single feed (two radiometers) or on a pair of feeds (four radiometers) according to the frequency (see the discussion in the previous section). The sensitivity corresponding to this case is reported as a "reference" in the first column of Table 3.

Again, a first sensitivity degradation factor $\sim \sqrt{2}$ with respect to Table 1 derives by considering only a single sky coverage and provides a lower limit to the sensitivity relevant here.

We have again to take into account the degradation factor $\sqrt{N_{ric,sky}}$ or $\sqrt{N_{ric,sky}/2}$ described in the previous section, according to the frequency.

We do not include in this case the last degradation factor, $\sim \sqrt{\rm FWHM/\Delta\theta_s}$, taking into account the possibility to lose the source after a given spin axis repointing. This is equivalent to consider variability times $\gtrsim 13$, 9, 6, 4 hours, respectively at 30, 44, 70 and 100 GHz; the worst sensitivity estimates reported in Table 2 are appropriate in the case of variability time-scales shorter than these.

Table 3: Instrumental noise estimates for variable sources.

| $\nu_{\rm eff}$/GHz | $\sigma_{\rm noise}$/mJy | $\sigma_{\rm noise}$/mJy | $\sigma_{\rm noise}$/mJy | $\sigma_{\rm noise}$/mJy | $\sigma_{\rm noise}$/mJy |
|---|---|---|---|---|---|
| Period $\rightarrow$ | 1 or 2 feed | $>$ 14 months | $\sim$ 14 months | 1–6 days/sin50° | $\sim$ few–12 hours/sin50° |
| Note $\rightarrow$ | worst case | auxiliary data | mission duration | 100 GHz wide ring | beam positions |
| 30 | 19.0 | 13.4 | 19.0 | – | – |
| 44 | 50.5 | 20.5 | 29.0 | – | 35.7÷50.0 |
| 70 | 68.6 | 28.0 | 39.6 | – | 68.6 |
| 100 | 188.0 | 32.2 | 45.5 | 71.0÷132.9 | 108.5÷132.9 |

Taking into account the above sensitivity degradation factors, the nominal PLANCK sensitivities relevant for variability studies on the indicated time-scales (longer than some hours) can be resumed in the ranges reported in Table 3. We report also in the table a comment that identifies the reason because we will be able study the variability on the corresponding time-scale. Table 4 provides also the useful number of independent measurements that we can extract from the data streams with the sensitivities quoted in Table 3 for the corresponding variability time-scales. If we are interested on variability time-scales longer than few years we can combine in a single measure the informations on a source obtained with the PLANCK data streams and compare it with the measures possibly acquired with other instruments before and after PLANCK observations. Note that during the mission we may find two or three source transits in the telescope field of view according to the source position in the sky (see column 3 of Table 4).

For sources located at $\theta_e$ significantly different from $\sim 50^\circ$ or $\sim 130^\circ$ the relevant sensitivities can be significantly different from those reported in Table 3, in particular at high absolute ecliptic latitudes. It is evident that the variability time-scales, $\tau$, for which the source location in the sky is crucial are those corresponding to the $5^{th}$ and $6^{th}$ column of Table 3 ($4^{th}$ and $5^{th}$ column of Table 4). Since the source crossing time-scale are $\propto 1/\sin\theta_e$, we can study source variability on time-scales in the range (1 – 6) days / $\sin\theta_e$ or (few hours – half day) / $\sin\theta_e$ with the same number of measurements reported in Table 4, but with sensitivity scaled by a factor $\sim \sqrt{\sin\theta_e/\sin 50^\circ}$. This should be advantageous in particular for weak sources, just above the detection limit from PLANCK time order data. For example, from this scaling law we derive a sensitivity improvement of a factor $\simeq 2$ at $\theta_e \simeq 10^\circ$ or $170^\circ$. The appropriate value may be somewhat different according to the detailed scanning strategy and beam position: for example, in the case of Figs. 1–3 we have an improvement by a factor $\simeq 2.5$. As a variance, for possible sources with fluxes significantly higher than the detection limit from PLANCK time order data it should be more advantageous to bin PLANCK data in numbers of useful observations larger than those reported in Table 4, with corresponding sensitivities scaled from those of Table 3 proportionally to the square root of the numbers of useful observations.

## 5 Conclusions

We have derived the PLANCK LFI sensitivity relevant for the study of moving objects and of variable sources from PLANCK time order data by properly rescaling the nominal sensitivity

Table 4: Number of useful measurements in the considered period.

| $\nu_{\rm eff}$/GHz<br>Period →<br>Note → | > 14 months<br>auxiliary data | ∼ 14 months<br>mission duration | 1–6 days/sin50°<br>100 GHz wide ring | ∼ few–12 hours/sin50°<br>beam positions |
|---|---|---|---|---|
| 30 | 1 | 2 (3) | – | – |
| 44 | 1 | 2 (3) | – | 2 |
| 70 | 1 | 2 (3) | – | 3 |
| 100 | 1 | 2 (3) | 6÷7 | 2÷3 |

of the final PLANCK maps.

According to the frequency channel, the kind of problem, the variability time-scales under consideration and the source position, they range in an interval between $\simeq$ 10 mJy and few $\times$ 100mJy.

The basic criteria to understand what values of sensitivity in the exploitation of the PLANCK time order data are appropriate to the different cases have been presented and discussed.

These sensitivity levels have to be compared to the sky confusion noise, or, in the hypothesis to be able to properly take advantage from MAP frequency maps, with the final MAP sensitivity, or, finally, with the final sensitivity of the PLANCK frequency maps, and have to be combined with them in order to evaluate the appropriate sensitivity relevant for each scientific case. The basic criteria for this kind of analysis have been presented.

**Acknowledgements.** It is a pleasure to thank M. Bersanelli, C.R. Butler, N. Mandolesi and F. Villa for interesting and useful discussions on PLANCK design and performances, G. De Zotti, L. Terenzi, L. Toffolatti and N. Vittorio for helpful and stimulating conversations on astrophysical and cosmological confusion noise and D. Maino for the long collaboration on the simulations of the PLANCK observations.

## References

[1] Burigana, C. et al., 2000, Int. Rep. ITeSRE 273/2000, April

[2] De Zotti, G. et al., 1999a, to appear in Proceedings of the Conference "3 K Cosmology", Roma, Italy, 5-10 October 1998, AIP Conference Proc, astro-ph/9902103

[3] De Zotti, G. et al., 1999b, New Astronomy, 4, 481

[4] Mandolesi, N. et al., 1998, PLANCK Low Frequency Instrument, A Proposal Submitted to the ESA

[5] Mather, J.C. et al., 1999, ApJ, 512, 511

[6] Puget, J. L. et al., 1998, High Frequency Instrument for the PLANCK Mission, A Proposal Submitted to the ESA

[7] Toffolatti, L. et al., 1998, MNRAS 297, 117

**Figure 1:** Full sky map of the sensititivy per pixel normalized to the average sensitivity in ecliptic coordinates. Note the elongated region with better sensitivity due to the triple sky coverage for a 14 months observation mission and the very high normalized sensitivity rings close to the ecliptic poles that contains unobserved regions [at $\theta_e$ less (larger) than 5° (175°)] due to the choice of 85° for the "scan angle" $\alpha$, i.e. the angle between the satellite spin axis and the telescope axis [here we have arbitrarily set to 0 the normalized sensitivity of the unobserved ecliptic polar caps for graphic purposes]. The map reported here properly refer to the case of a beam located along the line of sight of the PLANCK telescope with PLANCK is located in L2 and by assuming a simple scanning strategy. We assume that the observation will start three months after the launch date planned for February 15, 2007. Of course, the detailed sensitivity map for a given PLANCK beam depends on its position on the telescope field of view and on the details of the scanning strategy; on the other hand, the main pattern of the sensitivity map is in general similar to the map reported here.

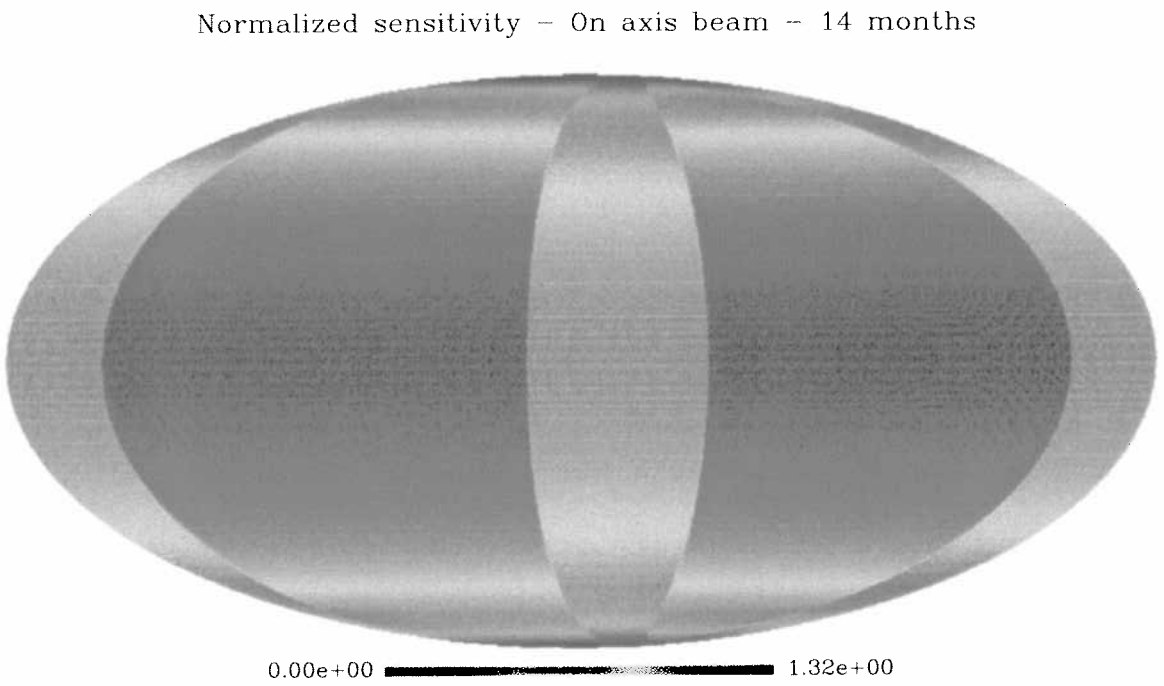

**Figure 2:** Normalized sensitivity averaged over the ecliptic longitudes as function of the ecliptic colatitude [we properly refer here to the sensitivity pattern of Fig. 1; see also the text and the caption of Fig. 1].

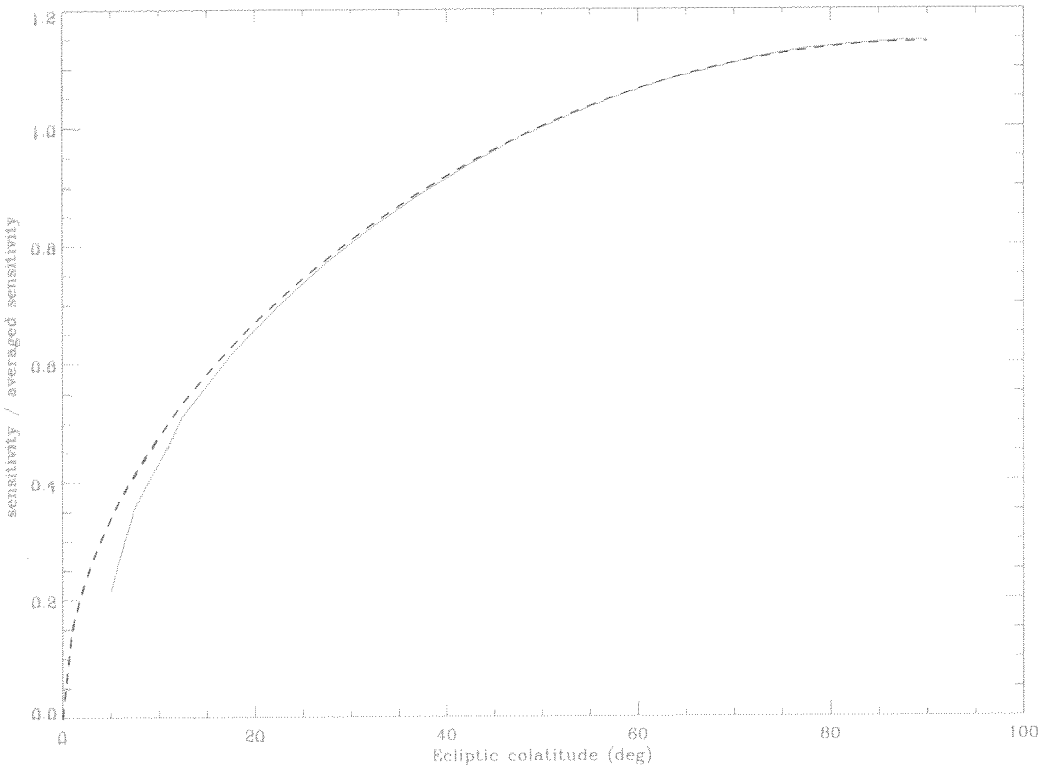

**Figure 3:** Fractions of sky with different values of the normalized sensitivity [we properly refer here to the sensitivity pattern of Fig. 1; see also the text and the caption of Fig. 1]. We bin here the normalized sensitivity at steps of $\pm 0.05$ about the values shown with the diamonds.

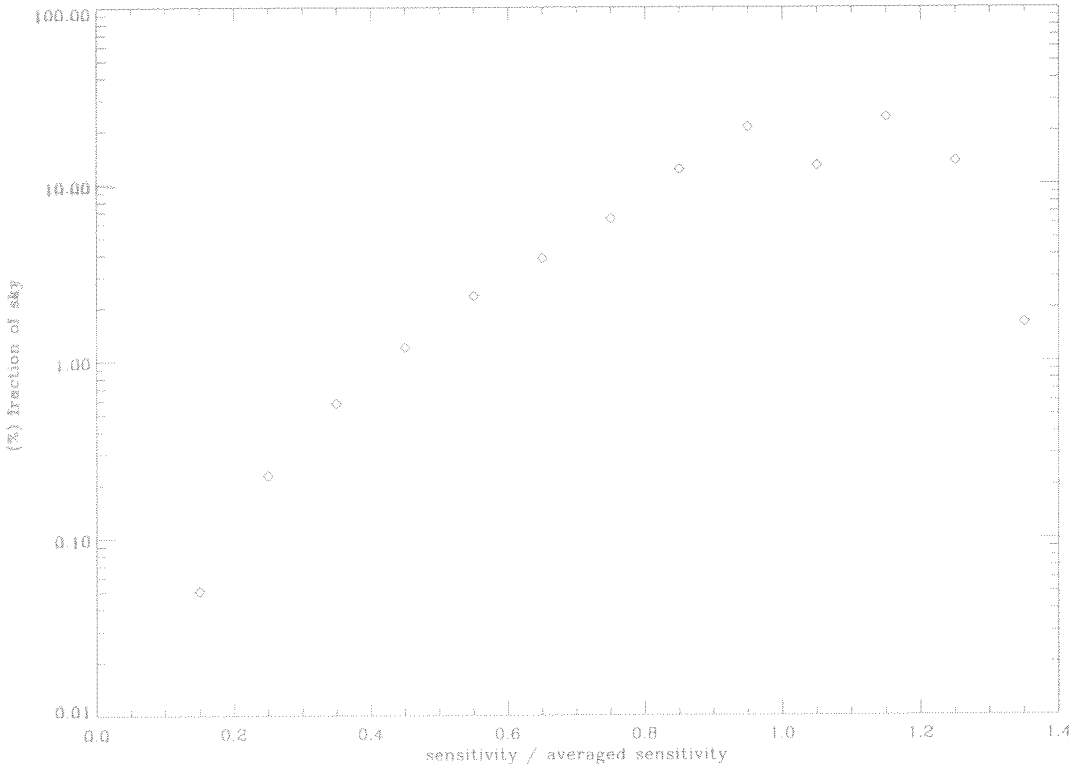

Figure 4: Position of LFI beams on the PLANCK telescope field of view. The two standard coordinates U and V on this plane are here multiplied by $180*60/\pi$ to be essentially angular distances expressed in arcminutes. For simple scanning strategies, the V direction identifies the direction of the sky scanning for each PLANCK scan circle whereas the U direction is parallel to the spin axis motion: it shifts by $2.5'$ / hour, i.e. $1^\circ$ / day. This determines the possible degradation of the PLANCK sensitivity for detecting moving or variable sources and the useful time periods for variability studies (see the text). Crosses: 100 GHz beams; stars: 70 GHz beams; rhombs: 44 Ghz beams; triangles: 30 GHz beams.